

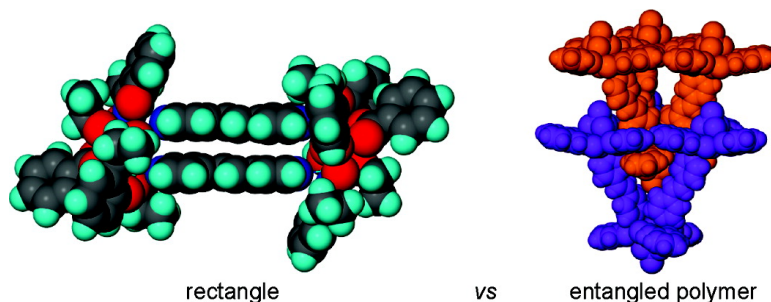
Communication

Supramolecular Entanglement from Interlocked Molecular Nanomagnets

Constantinos C. Stoumpos, Ross Inglis, Georgios Karotsis, Leigh F. Jones, Anna Collins, Simon Parsons, Constantinos J. Milios, Giannis S. Papaefstathiou, and Euan K. Brechin

Cryst. Growth Des., **2009**, 9 (1), 24-27 • DOI: 10.1021/cg800947z • Publication Date (Web): 04 December 2008

Downloaded from <http://pubs.acs.org> on January 8, 2009



More About This Article

Additional resources and features associated with this article are available within the HTML version:

- Supporting Information
- Access to high resolution figures
- Links to articles and content related to this article
- Copyright permission to reproduce figures and/or text from this article

[View the Full Text HTML](#)



ACS Publications
High quality. High impact.

Supramolecular Entanglement from Interlocked Molecular Nanomagnets

Constantinos C. Stoumpos,[†] Ross Inglis,[‡] Georgios Karotsis,[‡] Leigh F. Jones,[‡] Anna Collins,[‡] Simon Parsons,[‡] Constantinos J. Milios,^{‡,⊥} Giannis S. Papaefstathiou,^{*,§} and Euan K. Brechin^{*,‡}

Department of Chemistry, University of Patras, 360 04 Patras, Greece, School of Chemistry, The University of Edinburgh, West Mains Road, Edinburgh, EH9 3JJ, U.K., Department of Chemistry, University of Crete, Voutes 710 03, Herakleion Crete, Greece, and Laboratory of Inorganic Chemistry, Department of Chemistry, National and Kapodistrian University of Athens, Panepistimiopolis, 157 71 Zografou, Greece

Received August 27, 2008; Revised Manuscript Received November 12, 2008

ABSTRACT: The trinuclear nanomagnet $[\text{Mn}^{\text{III}}_3\text{O}(\text{Et-sao})_3(\text{MeOH})_3](\text{ClO}_4)$ (**1**) has been utilized as a building block for the construction of the hexanuclear cluster $[\{\text{Mn}^{\text{III}}_3\text{O}(\text{Et-sao})_3(\text{O}_2\text{CPh})(\text{EtOH})\}_2\{4,4'\text{-bpe}\}_2]$ (**3**) that conforms to a rectangle and the two-dimensional coordination polymer $\{[\text{Mn}^{\text{III}}_3\text{O}(\text{sao})_3(4,4'\text{-bpe})_{1.5}]\text{ClO}_4 \cdot 3\text{MeOH}\}_n$ (**2**·3MeOH). The latter exhibits an unprecedented type of entanglement that is based on host guest interactions. The polygon versus the polymer is rationalized in terms of changing an auxiliary anion that influences the arrangement of the potentially “vacant” coordination axes on each Mn^{III} ion of the trinuclear precursor and thereby directing the self-assembly process.

The potential of using molecular nanomagnets in applications such as information storage, molecular spintronics, and quantum computing has fuelled the synthesis and characterization of many beautiful molecules displaying fascinating physical properties.^{1–3} For example, the manganese single-molecule magnet (SMM) $[\text{Mn}_4\text{O}_3\text{Cl}_4(\text{O}_2\text{CET})_3(\text{py})_3]$, which crystallizes as a supramolecular hydrogen bonded dimer of cubanes $([\text{Mn}_4]_2)$,^{4,5} displays weak antiferromagnetic coupling between the two components resulting in quantum behavior different from that of the individual SMMs. This suggests a means of tuning quantum tunneling of magnetization (QTM) and opens the perspective that exchange coupled nanomagnets oriented in a controlled fashion through covalent or noncovalent interactions in one, two, and three dimensions may display fascinating physical properties.^{6–8}

We recently reported the synthesis and magnetic properties of a large family of hexanuclear and trinuclear Mn^{III} SMMs of general formulas $[\text{Mn}^{\text{III}}_6\text{O}_2(\text{R-sao})_6(\text{O}_2\text{CR})_2(\text{L})_{4–6}]$ and $[\text{Mn}^{\text{III}}_3\text{O}(\text{R-sao})_3(\text{O}_2\text{CR})(\text{L})_3]$ ($\text{saoH}_2 = \text{salicylaldoxime}$; $\text{R} = \text{H}, \text{Me}, \text{Et}, \text{etc}$; $\text{L} = \text{solvent}$),^{9–12} the latter being the analogous “half” molecules of the former.¹³ We showed in each case that by using derivatized versions of the oxime ligand it was possible to significantly increase the ground spin state from $S = 4$ to $S = 12$ in the former and from $S = 2$ to $S = 6$ in the latter, enhancing the effective energy barrier for magnetization reversal to record levels.^{9–11} The origin of the $\text{AF} \rightarrow \text{F}$ switch arises from a structural distortion of the molecule induced by the “twisting” of the $(-\text{Mn}-\text{N}-\text{O}-)_3$ ring, as evidenced by the significant increases in the $\text{Mn}-\text{N}-\text{O}-\text{Mn}$ torsion angles observed when bulkier salicylaldoximes are employed.¹²

Here we present our first attempts to exploit such magnetic clusters as building blocks for the formation of supramolecular architectures (i.e., polygons, polyhedra, and polymeric arrays)¹⁴ by means of coordination-driven self-assembly.^{15,16} Specifically, the combination of the trinuclear cluster hereafter denoted as $[\text{Mn}_3]$ with the linear bridging ligand *trans*-1,2-bis(4-pyridyl)ethylene (4,4'-bpe) gives rise to both a polygon and a two-dimensional (2D) coordination polymer, with the latter exhibiting an unprecedented

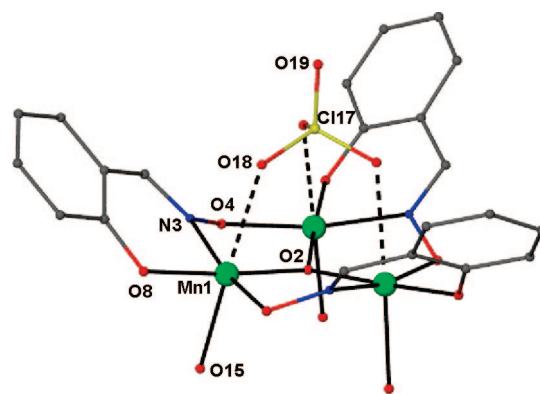


Figure 1. The molecular structure of complex **1**. Color code: Mn green, O red, N blue, Cl yellow, C gray. The H-atoms and some of the C-atoms have been removed for clarity.

type of entanglement.¹⁷ The polygon versus the polymer is rationalized in terms of changing an auxiliary anion that influences the arrangement of the potentially “vacant” coordination axes on each Mn^{III} ion of the $[\text{Mn}_3]$ precursor and thereby directing the self-assembly process.

The $[\text{Mn}_3]$ precursor was synthesized by reacting $\text{Mn}(\text{ClO}_4)_2 \cdot 6\text{H}_2\text{O}$ and Et-saoH_2 in MeOH in the presence of a Et_4NOH . X-ray quality crystals of $[\text{Mn}^{\text{III}}_3\text{O}(\text{Et-sao})_3(\text{MeOH})_3](\text{ClO}_4)$ ($[\text{Mn}_3]$, **1**) ($\text{Et-saoH}_2 = \text{ethyl-salicylaldoxime}$) were obtained in approximately 30% yield. Complex **1**¹⁸ (Figure 1) crystallizes in the rhombohedral space group $R\bar{3}$ and consists of a $[\text{Mn}^{\text{III}}_3(\mu_3\text{-O})]^{7+}$ triangular unit with the three Et-sao^{2-} ligands bridging in a $\eta^1:\eta^1:\eta^1:\mu$ -fashion along the edges of the $[\text{Mn}_3]$ core. A 3-fold inversion axis which is perpendicular to the $[\text{Mn}_3]$ mean plane passes through the central $\mu_3\text{-O}^{2-}$ ($\text{O}2$), the perchlorate chlorine atom ($\text{Cl}17$), and one of the ClO_4^- oxygen atoms ($\text{O}19$). A MeOH molecule is attached to each Mn^{III} ion, with all three being oriented on the same side of the triangular unit which is further capped by a $\eta^1:\eta^1:\eta^1:\mu_3$ weakly coordinated ClO_4^- anion [$\text{Mn}1-\text{O}18 = 2.550 \text{ \AA}$] on the opposite side. In this arrangement, each Mn^{III} ion adopts a distorted octahedral geometry and displays Jahn–Teller (JT) elongation, as expected for high-spin $3d^4$ ions in near octahedral geometry. The central $\mu_3\text{-O}^{2-}$ ion deviates by about 0.18 \AA from the $[\text{Mn}_3]$ plane toward the terminally bound MeOH molecules, while the phenyl

* Authors to whom correspondence should be addressed. E-mail: gspapaef@chem.uoa.gr. Fax: 30-210-727-4782 (G.S.P.). E-mail: ebrechin@staffmail.ed.ac.uk. Fax: 44-131-650-6453 (E.K.B.).

[†] University of Patras.

[‡] University of Edinburgh.

[⊥] University of Crete.

[§] University of Athens.

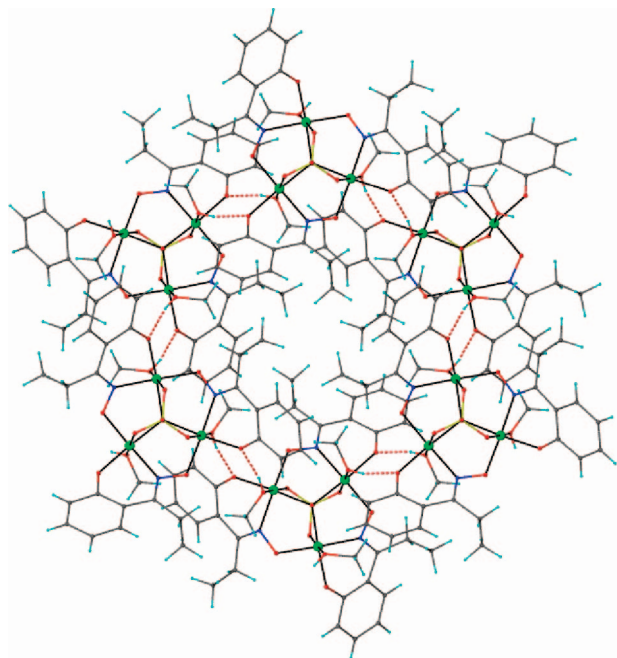


Figure 2. Part of the (6,3) hydrogen-bonded framework of **1**.

groups of the Et-sao²⁻ ligands are twisted toward the perchlorate. Due to the presence of the capping ClO₄⁻ anion, the JT axes of the Mn^{III} ions [O18–Mn1–O15_{MeOH}] are not parallel and form an angle of about 22.4° to each other and an angle of about 12.96° to the [Mn₃] plane converging toward the ClO₄⁻ anion. Each [Mn₃] unit forms three complementary hydrogen bonds with three other [Mn₃] units that involve the coordinated MeOH molecules and the phenolate oxygen atoms of the Et-sao²⁻ ligands [O15–H1⋯O8 = 2.734 Å] giving rise to an undulated 2D hydrogen bonded framework with a (6,3) topology running parallel to the *ab* plane (Figure 2).

Having in mind the principles of coordination-driven self-assembly and examining the crystal structure of **1**, we reasoned that an attempt to exchange the MeOH molecules with a linear bridging ligand such as 4,4'-bpe could not lead to a discrete architecture since the elongation axes on the Mn^{III} ions diverge on that side of the molecule.¹⁵ Indeed, upon addition of a CH₂Cl₂ solution of 4,4'-bpe to a methanolic solution of Mn(ClO₄)₂·6H₂O and saoH₂, a dark green solution formed from which dark green prismatic crystals of {[Mn^{III}₃O(sao)₃(4,4'-bpe)_{1.5}]ClO₄·3MeOH}_n ([Mn₃]_n, 2·3MeOH) formed in about 30% yield. Complex **2**¹⁸ crystallizes in the trigonal space group *P*3̄c and consists of μ-oxo-centered [Mn^{III}₃O(sao)₃]ClO₄ units and 4,4'-bpe molecules (Figure 3). The components have assembled to form a 2D coordination polymer where the 4,4'-bpe molecules bridge the [Mn₃] units. The ligation of the sao²⁻ and the ClO₄⁻ anions around the [Mn₃] unit in **2** is similar to **1**. A 3-fold axis passes through the central μ₃-O²⁻ (O2), the ClO₄⁻ chlorine atom (Cl20) and one of the perchlorate oxygen atoms (O22) and is perpendicular to the [Mn₃] plane. The Mn^{III} ions are in axially elongated octahedral environments with the JT axes [O21–Mn1–N13] again converging toward the ClO₄⁻ side and diverging toward the 4,4'-bpe side of the [Mn₃] cluster forming an angle of 26.29° to each other and an angle of 15.22° to the [Mn₃] plane. Compared to **1**, the JT axes in **2** have become more profoundly inclined, to accommodate the larger 4,4'-bpe molecules as compared to the MeOH molecules in **1**. As a result, the central μ₃-O²⁻ ion deviates by 0.303 Å from the [Mn₃] plane toward the 4,4'-bpe molecules.

The 2D network adopted by **2** conforms to a (6,3) regular net with the [Mn₃] units acting as three-connected nodes (Figure 4). Due to the peculiar shape of the [Mn₃] unit which is nearly flat and the orientation of the connection sites on the [Mn₃] cluster

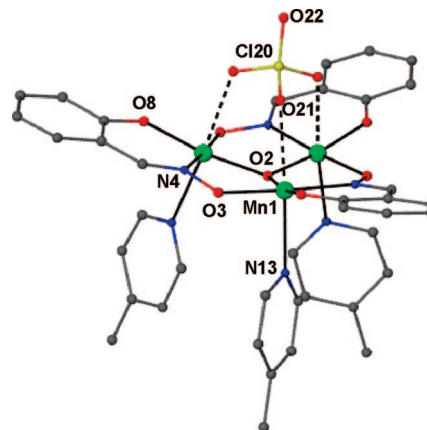


Figure 3. The trinuclear unit of complex **2**. Color code as in Figure 1.

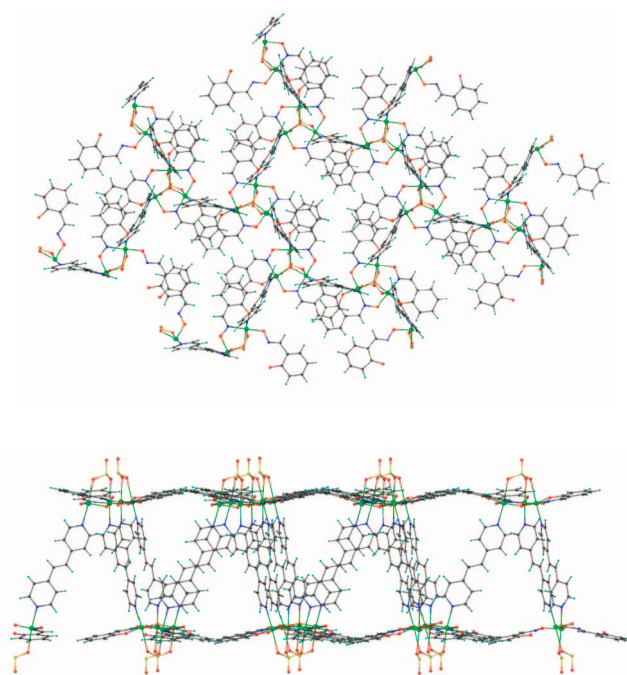


Figure 4. Top and side (bottom) views of the 2D (6,3)-net of **2**.

which are all pointing toward the same side of the [Mn₃] plane and converging toward the ClO₄⁻ side, the 2D network is highly distorted such that the [Mn₃] units are placed alternately above and below the mean plane of the 2D net. This arrangement gives rise to the formation of conical cavities within the body of the 2D framework, which is approximately 12.6 Å thick. The upper rims of the conical cavities point alternately above and below the plane of the net such that half of the rims of the cavities point above and half below the layer. Each cavity is composed of a [Mn₃] unit, which serves as the bottom of the cavity and three 4,4'-bpe molecules, while three other [Mn₃] units from the same net are attached to each of the three 4,4'-bpe molecules narrowing the “gates” of the cavities’ rims.

A salient feature of the structure of **2** is that the size of each {[Mn₃](4,4'-bpe)₃[Mn₃]₃} cavity is large enough to host a [Mn₃] unit of an adjacent net (Figures 5 and 6). This host–guest interaction is further supported by three hydrogen-bonding interactions that involve one of the beta C–H groups of the three cavity forming 4,4'-bpe molecules and the uncoordinated oxygen atom of the ClO₄⁻ that caps the [Mn₃] guest [C15–H151⋯O22 = 3.363 Å]. The [Mn₃] guest is in an eclipse orientation with respect to the [Mn₃] at the bottom of the host cavity while the three [Mn₃] units at the

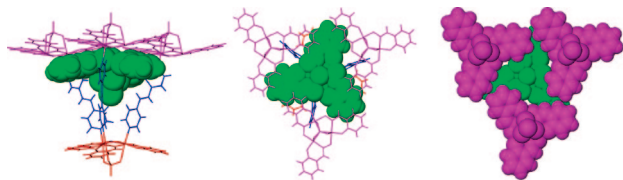


Figure 5. Side (left) and top (right) views of the $[\text{Mn}_3]\text{C}\{[\text{Mn}_3](4,4'\text{-bpe})_3[\text{Mn}_3]_3\}$.

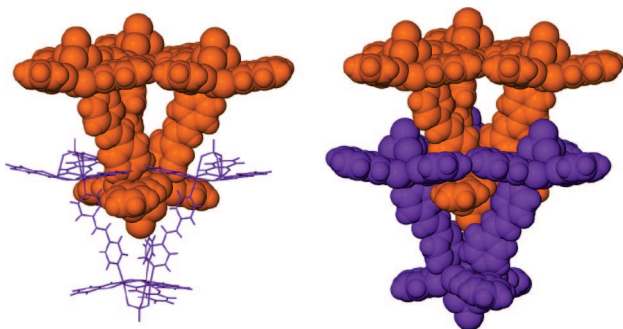


Figure 6. Views of an ice-cream cone within an ice-cream cone.

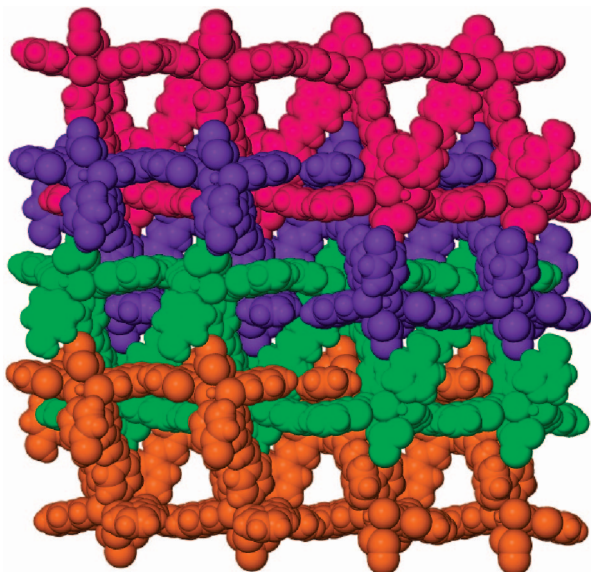


Figure 7. View of the entangled layers of **2**.

rim's gate of the conical cavity prohibit the $[\text{Mn}_3]$ guest from exiting (Figure 5). Therefore, each $[\text{Mn}_3]$ serves as (i) the bottom for the conical cavity, (ii) one of the gate-keepers of a neighboring cavity while (iii) acting as the guest for a cavity belonging to a neighboring net.

Each layer is interlocked with two other layers, one above and one below the middle layer's plane, resulting in an entangled array with an increased dimensionality (i.e., from 2D to 3D) (Figure 7). This interlocking is purely supramolecular in nature since it is based on host–guest and hydrogen bonding interactions as described above. Each layer acts as a host and at the same time as a guest to both neighboring layers. In principle the layers of **2** could be disentangled by stretching out but that is prohibited since it is impossible to have the 4,4'-bpe molecules and the $[\text{Mn}_3]$ units in the same plane due to the orientation of the connection sites on the $[\text{Mn}_3]$ units. From the topological point of view, the interlocking of the 2D layers of **2** does not belong to any known type of entanglement.^{17,19–21} Topological entanglement (i.e., interpenetration and polycatenation) is easily excluded since (i) the dimen-

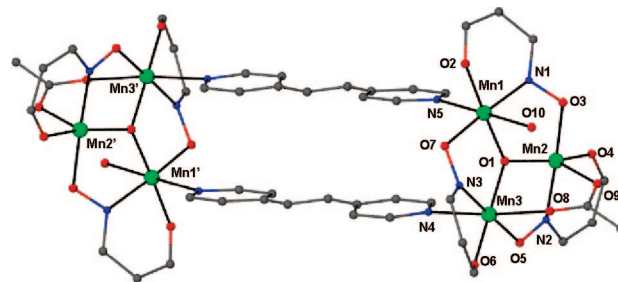


Figure 8. The rectangular hexanuclear assembly of **3**. Color code as in Figure 1. The H-atoms and some of the C-atoms have been removed for clarity.

sionality in **2** increases due to the entanglement, (ii) no bond-breaking is required to disentangle the layers, thus excluding interpenetration²⁰ and (iii) the closed circuits [i.e., the hexagonal rings of the (6,3) net of **2**] are not catenated (i.e., do not form Hopf or Borromean links), thus excluding polycatenation.²¹ Euclidean entanglement^{17,19} (i.e., polythreading) can also be excluded since none of the closed loops [i.e., the hexagonal circuits of the (6,3) net of **2**] are threaded. That the layers of **2** form cavities to host the $[\text{Mn}_3]$ units of neighboring layers resulting in an architecture of increased dimensionality means that this is a new type of a supramolecular entanglement where real host–guest interactions are responsible for the interlocking (Figures 6 and 7).

In order to prove that the capping $\mu_3\text{-ClO}_4^-$ is responsible for inducing the symmetry that led to the formation of **2**, we decided to change it for another anion that could not coordinate to all three Mn^{III} ions, thus releasing the coordination axes on the $[\text{Mn}_3]$ unit from converging toward the same direction with respect to the $[\text{Mn}_3]$ plane. By treating $\text{Mn}(\text{PhCO}_2)_2 \cdot 2\text{H}_2\text{O}$ with Et-saoH_2 and 4,4'-bpe in EtOH in the presence of Et_4NOH , X-ray quality crystals of $[\{\text{Mn}^{\text{III}}_3\text{O}(\text{Et-sao})_3(\text{O}_2\text{CPh})(\text{EtOH})\}_2\{4,4'\text{-bpe}\}_2]$ ($[\text{Mn}_3]_2$, **3**) were obtained in ~30% yield. The same product can be derived from the reaction of an ethanolic solution of $[\text{Mn}^{\text{III}}_6\text{O}_2(\text{Et-sao})_6(\text{O}_2\text{-CPh})_2(\text{EtOH})_4(\text{H}_2\text{O})_2]$ with 4,4'-bpe in ~25% yield. A view of the crystal structure of **3**¹⁸ reveals that two trinuclear $[\text{Mn}^{\text{III}}_3\text{O}(\text{Et-sao})_3(\text{O}_2\text{CPh})(\text{EtOH})]$ units assemble with two 4,4'-bpe molecules to form a hexanuclear rectangular assembly, sustained by four $\text{Mn-N}_{4,4'\text{-bpe}}$ bonds (Figure 8). An inversion center in the middle of the molecule correlates the two $[\text{Mn}_3]$ units. The two 4,4'-bpe molecules are organized between the two $[\text{Mn}_3]$ clusters in a face-to-face stacked arrangement and separated by 3.5 Å, thus qualifying the $[\text{Mn}_3]$ cluster as a linear template.^{16,22} The ligation of the Et-sao^{2-} around the $[\text{Mn}_3]$ unit in **3** is similar to **1** and **2**. Two phenyl groups of two Et-sao^{2-} ligands are twisted toward the 4,4'-bpe side with the third pointing to the other direction. Two of the three Mn^{III} ions are in distorted octahedral environments with the third adopting a square pyramidal geometry. The capping $\mu_3\text{-ClO}_4^-$ in **1** and **2** has been replaced by a *syn,syn-μ-PhCO}_2^-* and a terminal EtOH molecule.

The ligation of the PhCO_2^- and the EtOH molecules has destroyed the 3-fold inversion axis, present in **1** and the 3-fold axis present in **2**, thus releasing the JT axes on the Mn^{III} ions from converging toward the same side of the $[\text{Mn}_3]$ plane. The Mn^{III} ions that coordinate to the 4,4'-bpe molecules are those in the octahedral environment, with the oxygen atoms from a PhCO_2^- and an EtOH molecule on the apical positions against the nitrogen atoms (N4 and N5) of the 4,4'-bpe molecules. The JT axes on those Mn^{III} ions are inclined to each other by an angle of 19.13° [$\text{O10-Mn1-N5}\angle\text{O8-Mn3-N4}$], thus being more twisted compared with the analogous axes in **1** and **2**, but they do not converge toward the PhCO_2^- and the EtOH as they did in **1** and **2**. The distortion implied by the different set of auxiliary ligands (i.e., PhCO_2^- and EtOH) to the same side of the $[\text{Mn}_3]$ plane is evidenced by the deviation of 0.274 Å of the central $\mu_3\text{-O}^{2-}$ ion from the $[\text{Mn}_3]$ plane which is in between the analogous deviation in **1** and

2. Therefore, the replacement of the ClO_4^- ligands by a PhCO_2^- and the EtOH molecule in **3** has lowered the local symmetry around the $[\text{Mn}_3]$ cluster giving rise to a polygon (i.e., a rectangle) instead of a coordination polymer as in **2**. Alternatively, **3** might be described as a “dimer of clusters” or a “pair of clusters”²³ which is a rather new perspective of looking at how magnetic clusters can be arranged in the crystal lattice with respect to each other.²⁴

In this report, the molecular nanomagnet $[\text{Mn}_3]$ has been utilized as a building block for the construction of supramolecular architectures. By applying the principles of coordination-driven self-assembly we have isolated a 2D coordination polymer (i.e., $[\text{Mn}_3]_n$) that exhibits a novel type of a supramolecular entanglement which is based on host–guest interactions and increases the dimensionality of the bulk material to 3D and a polygon (i.e., $[\text{Mn}_3]_2$). The polygon versus the polymer was rationalized in terms of changing the capping ClO_4^- that forces the connection coordination axes on each Mn^{III} ion of the $[\text{Mn}_3]$ precursor to converge toward its side by a PhCO_2^- and an EtOH molecule that lower the local symmetry around the $[\text{Mn}_3]$, releasing the JT connection axes and therefore directing the self-assembly process.

Acknowledgment. The authors gratefully acknowledge the EPSRC and Leverhulme Trust (UK). GSP thanks the Special Account for Research Grants (SARG) of the National and Kapodistrian University of Athens for support. The work was also supported by MAGMANet (NMP3-CT-2005-515767).

Supporting Information Available: Crystallographic data of complexes **1**, **2**, and **3** as CIF files (also available as CCDC reference numbers 696165, 696166, and 696167). This material is available free of charge via the Internet at <http://pubs.acs.org>.

References

- Gatteschi, D.; Sessoli, R. *Angew. Chem., Int. Ed.* **2003**, *42*, 268.
- Gatteschi, D.; Sessoli, R.; Villain, J. *Molecular Nanomagnets*; Oxford University Press: New York, 2007, and references therein.
- Aromi, G.; Brechin, E. K. *Struct. Bonding (Berlin)* **2006**, *122*, 1, and references therein.
- Wernsdorfer, W.; Aliaga-Alcalde, N.; Hendrickson, D. N.; Christou, G. *Nature* **2002**, *416*, 406.
- Hill, S.; Edwards, R. S.; Aliaga-Alcalde, N.; Christou, G. *Science* **2003**, *302*, 1015.
- Boskovic, C.; Bircher, R.; Tregenna-Piggott, P. L. W.; Güdel, H. U.; Paulsen, C.; Wernsdorfer, W.; Barra, A.-L.; Khatsko, E.; Neels, A.; Stoeckli-Evans, H. *J. Am. Chem. Soc.* **2003**, *125*, 14046.
- Yoo, J.; Wernsdorfer, W.; Yang, E.-C.; Nakano, M.; Rheingold, A. L.; Hendrickson, D. N. *Inorg. Chem.* **2005**, *44*, 3377.
- Miyasaka, H.; Nakata, K.; Lecren, L.; Coulon, C.; Nakazawa, Y.; Fujisaki, T.; Sugiura, K.; Yamashita, M.; Clérac, R. *J. Am. Chem. Soc.* **2006**, *128*, 3770.
- Milios, C. J.; Vinslava, A.; Wood, P. A.; Parsons, S.; Wernsdorfer, W.; Christou, G.; Perlepes, S. P.; Brechin, E. K. *J. Am. Chem. Soc.* **2007**, *129*, 8.
- Milios, C. J.; Vinslava, A.; Moggach, S.; Parsons, S.; Wernsdorfer, W.; Christou, G.; Perlepes, S. P.; Brechin, E. K. *J. Am. Chem. Soc.* **2007**, *129*, 2754.
- Milios, C. J.; Vinslava, A.; Wernsdorfer, W.; Prescimone, A.; Wood, P. A.; Parsons, S.; Perlepes, S. P.; Christou, G.; Brechin, E. K. *J. Am. Chem. Soc.* **2007**, *129*, 6547.
- Milios, C. J.; Inglis, R.; Vinslava, A.; Bagai, R.; Wernsdorfer, W.; Parsons, S.; Perlepes, S. P.; Christou, G.; Brechin, E. K. *J. Am. Chem. Soc.* **2007**, *129*, 12505.
- (a) Milios, C. J.; Piligkos, S.; Brechin, E. K. *Dalton Trans.* **2008**, 1809. (b) Cano, J.; Cauchy, T.; Ruiz, E.; Milios, C. J.; Stoumpos, C. C.; Stamatatos, T. C.; Perlepes, S. P.; Christou, G.; Brechin, E. K. *Dalton Trans.* **2008**, 234. (c) Milios, C. J.; Brechin, E. K. *Polyhedron* **2007**, *26*, 1927.
- (a) Holliday, B. J.; Mirkin, C. A. *Angew. Chem., Int. Ed.* **2001**, *40*, 2022. (b) Fujita, M.; Umemoto, K.; Yoshizawa, M.; Fujita, N.; Kusukawa, T.; Biradha, K. *Chem. Commun.* **2001**, 509. (c) Fyfe, M. C. T.; Stoddart, J. F. *Acc. Chem. Res.* **1997**, *30*, 393. (d) Swiegers, G. F.; Malefsete, T. J. *Chem. Eur. J.* **2001**, *7*, 3636. (e) Calder, D. L.; Raymond, K. N. *Acc. Chem. Res.* **1999**, *32*, 975. (f) Yaghi, O. M.; O’Keeffe, M.; Ockwig, N. W.; Chae, H. K.; Eddaoudi, M.; Kim, J. *Nature* **2003**, *423*, 705. (g) Moulton, B.; Zaworotko, M. J. *Chem. Rev.* **2001**, *101*, 1629. (h) Kitagawa, S.; Kitaura, R.; Noro, S. *Angew. Chem., Int. Ed.* **2004**, *43*, 2334. (i) Hosseini, M. W. *Acc. Chem. Res.* **2005**, *38*, 313. (j) Hosseini, M. W. *Chem. Commun.* **2005**, 5825.
- (a) Stang, P. J. *Chem. Eur. J.* **1998**, *4*, 19. (b) Seidel, S. R.; Stang, P. J. *Acc. Chem. Res.* **2002**, *35*, 972.
- (a) Papaefstathiou, G. S.; Zhong, Z.; Geng, L.; MacGillivray, L. R. *J. Am. Chem. Soc.* **2004**, *126*, 9158. (b) Papaefstathiou, G. S.; Georgiev, I. G.; Friscic, T.; MacGillivray, L. R. *Chem. Commun.* **2005**, 3974.
- Carlucci, L.; Ciani, G.; Proserpio, D. M. *Coord. Chem. Rev.* **2003**, *246*, 247.
- Diffraction data were collected with Mo-K α radiation ($\lambda = 0.71073$ Å) on a Bruker Smart Apex CCD Diffractometer. Crystal Data for **1**: $\text{C}_{30}\text{H}_{39}\text{N}_3\text{O}_{14}\text{ClMn}_3$, $M = 865.89$, black square, trigonal, $R\bar{3}$, $a = 13.3784(3)$, $b = 13.3784(3)$, $c = 34.0617(12)$ Å, $\alpha = \beta = 90.0$, $\gamma = 120.0$, $V = 5279.7(3)$ Å³, 63184 reflections collected of which 3607 were independent ($R_{\text{int}} = 0.036$), 154 parameters and 0 restraints, $R1 = 0.0288$ [based on $I > 2\sigma(I)$], $wR2 = 0.0679$ (all data). Crystal Data for **2**: $\text{C}_{39}\text{H}_{30}\text{N}_6\text{O}_{11}\text{Mn}_3(4\text{CH}_3\text{OH})$, $M = 1055.07$, black block, trigonal, $P\bar{3}1c$, $a = 15.6887(3)$, $b = 15.6887(3)$, $c = 22.2702(8)$ Å, $\alpha = \beta = 90$, $\gamma = 120$, $V = 4747.1(2)$ Å³, 21939 reflections collected of which 4188 were independent ($R_{\text{int}} = 0.075$), 181 parameters and 0 restraints, $R1 = 0.0666$ [based on $I > 2\sigma(I)$], $wR2 = 0.1807$ (all data). Crystal Data for **3**: $\text{C}_{96}\text{H}_{94}\text{Mn}_6\text{N}_{10}\text{O}_{20}$, $M = 2037.43$, black block, monoclinic, $P2_1/n$, $a = 13.4841(4)$, $b = 18.4592(5)$, $c = 19.6489(6)$ Å, $\alpha = \gamma = 90$, $\beta = 104.358(2)$, $V = 4738.0(2)$ Å³, 70341 reflections collected of which 12809 were independent ($R_{\text{int}} = 0.059$), 583 parameters and 54 restraints, $R1 = 0.0717$ [based on $I > 2\sigma(I)$], $wR2 = 0.1737$ (all data).
- Hyde, S. T.; Larsson, A.-K.; Matteo, T. D.; Ramsden, S.; Robins, V. *Aust. J. Chem.* **2003**, *56*, 981.
- (a) Batten, S. R. *CrystEngComm* **2001**, *18*, 1. (b) Batten, S. R.; Robson, R. *Angew. Chem., Int. Ed.* **1998**, *37*, 1460. (c) Baburin, I. A.; Blatov, V. A.; Carlucci, L.; Ciani, G.; Proserpio, D. M. *J. Solid State Chem.* **2005**, *178*, 2452. (d) Blatov, V. A.; Carlucci, L.; Ciani, G.; Proserpio, D. M. *CrystEngComm* **2006**, *6*, 377.
- (a) Carlucci, L.; Cianni, G.; Proserpio, D. M. *CrystEngComm* **2003**, *5*, 269. (b) Sauvage, J.-P. *Acc. Chem. Res.* **1998**, *31*, 611. (c) Raymo, F. M.; Stoddart, J. F. *Chem. Rev.* **1999**, *99*, 1643. (d) Nepogodiev, S. A.; Stoddart, J. F. *Chem. Rev.* **1998**, *98*, 1959.
- (a) MacGillivray, L. R.; Papaefstathiou, G. S.; Friscic, T.; Hamilton, T. D.; Bucar, D.-K.; Chu, Q.; Varshney, D. B.; Georgiev, I. G. *Acc. Chem. Res.* **2008**, *41*, 280. (b) MacGillivray, L. R.; Papaefstathiou, G. S.; Friscic, T.; Varshney, D. B.; Hamilton, T. D. *Top. Curr. Chem.* **2004**, *248*, 201.
- (a) Sanudo, E. C.; Cauchy, T.; Ruiz, E.; Laye, R. H.; Roubeau, O.; Teat, S. T.; Aromi, G. *Inorg. Chem.* **2007**, *46*, 9045. (b) Knapp, M. J.; Hendrickson, D. N.; Grillo, V. A.; Bollinger, J. C.; Christou, G. *Angew. Chem., Int. Ed. Engl.* **1996**, *35*, 1818.
- Roubeau, O.; Clérac, R. *Eur. J. Inorg. Chem.* **2008**, 4325.

CG800947Z